Surface Chemistry

DOI: 10.1002/anie.201309415

Controlled Carbon Nitride Growth on Surfaces for Hydrogen Evolution Electrodes**

Menny Shalom, Sixto Gimenez, Florian Schipper, Isaac Herraiz-Cardona, Juan Bisquert, and Markus Antonietti*

Abstract: *Efficient and low-cost electrocatalysts for the hydrogen evolution reaction are highly desired for future renewable energy systems. Described herein is the reduction of water to hydrogen using a metal-free carbon nitride electrocatalyst which operates in neutral and alkaline environments. An efficient, easy, and general method for growing ordered carbon nitride on different electrodes was developed. The metal-free catalyst demonstrates low overpotential values, which are comparable to those of non-noble metals, with reasonable current densities. The facile deposition method enables the fabrication of many electronic and photoelectronic devices based on carbon nitride for renewable energy applications.*

Production of hydrogen from water has been attracting a lot of attention because of the possibility of generating a clean energy carrier without CO_2 emissions, as well as opportunities in the field of energy storage.[1] The electrocatalytic production of hydrogen from water demands the use of a catalyst which can generate hydrogen with minimal overpotential.[2] Up to now only metals, such as the noble metal platinum, have been used as the catalyst because of the fast kinetics for driving this reaction with low overpotential.[3] However, the high price and the critical abundance of noble metals motivate intense research of non-noble metals and metal composite materials for the hydrogen evolution reaction (HER). Several non-noble metal materials, such as transition-metal nitrides,[4] carbides,[5] and complexes, along with metal alloys[6] have been investigated as catalysts for hydrogen evolution from water.[7] However, despite great progress in finding new materials as catalysts, and to the knowledge of the authors, all of the catalysts for HERs contain a metal center which is essential for this reaction.

In recent years, carbon nitride (simplified as C_3N_4) has appeared to be a good metal-free catalyst in many energy-related applications.[8] Carbon nitride materials demonstrated high activity in heterogeneous catalysis,[9] photocatalysis,[10] photodegradation of pollutants,[11] oxygen reduction reactions,[12] and many more.[13] Carbon nitride synthesis usually involves the thermal condensation of organic molecules which contain nitrogen and carbon atoms (i.e., cyanamide, melamine, urea, etc.), and results in lowly organized C_3N_4 textures with small grain sizes.[14] Moreover, because of the nature of C_3N_4 synthesis, the resulting C_3N_4 possesses low surface area, low conductivity, and poor electronic properties. In contrast, the chemical and physical properties of carbon nitride can be easily modified by using templating methods,[15] the insertion of different heteroatoms[16] and molecules within its structure, and other chemical tools.[17a] Consequently, many applied modifications of C_3N_4 materials resulted in the improvement of their chemical, electronic, and catalytic properties. Nevertheless, all the above modifications are solely related to C_3N_4 in its powder form, whereas, for electrochemical applications such as fuel cells and water electrosplitting, a direct connection between C_3N_4 and the conductive materials must be established. Because of the large particle size and the insolubility of C_3N_4 in most solvents, the use of common deposition techniques such as spin-coating and screen-printing results in poor coverage and conductivity.[17b,18] Recently, it was shown that by using nanocasting techniques, carbon nitride could be inserted into highly ordered porous carbon[12b] or into graphene-based mesoporous silica nanosheets[19] for conductivity improvement. These methods improve the dispersion and the conductivity of the composite materials toward C_3N_4 utilization as a catalyst in fuel cells. Nevertheless, for direct (photo) electrochemical measurements of C_3N_4 as an electrocatalyst (i.e., water splitting) or for photoelectric measurements, it is essential to find a new and simple synthetic pathway to grow C_3N_4 on different substrates.

Recently, Thomas et al.[20] and our group[11a] demonstrated the utilization of the hydrogen-bonded cyanuric acid melamine (CM) supramolecular complex as a new and simple synthetic way to form ordered structures of carbon nitride. Beside its hydrogen bonds, the CM complex possesses free hydroxy and amine groups which can be attached to different substrates. On this basis, we present here a generic, facile, and easy method to grow highly ordered carbon nitride on different substrates from surface-bound CM complexes, and demonstrate the high suitability of this material to catalyze the HERs. The applied protocol results in the deposition of ordered C_3N_4 rods, with enhanced surface area, on glass and fluorine-doped tin oxide (FTO) with respect to the bulk C_3N_4. Moreover, we show that C_3N_4 can also be easily grown on porous metal oxide electrodes (TiO_2, ZnO, etc.). The chemical structure, morphology, and optical properties of

[*] Dr. M. Shalom, F. Schipper, Prof. Dr. M. Antonietti
Department of Colloid Chemistry
Max Planck Institute of Colloids and Interfaces
Research Campus Golm, 14424 Potsdam (Germany)
E-mail: menny.shalom@mpikg.mpg.de
Dr. S. Gimenez, I. Herraiz-Cardona, Prof. J. Bisquert
Departament de Física
Photovoltaics and Optoelectronic Devices Group
Universitat Jaume I, 12071 Castelló (Spain)

[**] M.S. thanks "Minerva Fellowship" for financial support and Dr. Laurent Chabanne for fruitful discussions.

Supporting information for this article is available on the WWW under http://dx.doi.org/10.1002/anie.201309415.

the resulting films were characterized by XRD, FTIR, scanning electron microscopy (SEM), energy-dispersive X-ray (EDX) spectroscopy, elemental analysis (EA), UV/Vis absorption, and emission spectra. The electrochemical properties of C_3N_4 on FTO and TiO_2 were evaluated by a cyclic voltammetry method in neutral and basic media. The method for depositing carbon nitride on different substrates is schematically shown in Figure 1.

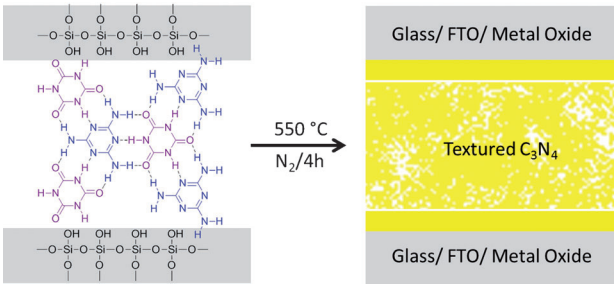

Figure 1. Illustration of the synthetic procedure for depositing carbon nitride on different substrates (for simplification, only glass is shown).

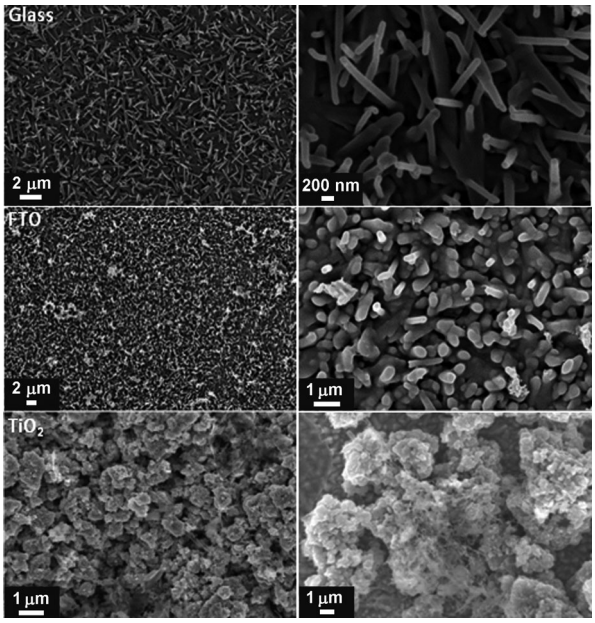

Figure 2. SEM images of carbon nitride deposited on glass, FTO, and TiO_2.

The supramolecular complex was prepared by simple mixing of a 1:1 cyanuric acid and melamine mixture in water, as previously described.[11a] A thin layer of the solid complex was placed between the two desired substrates and the electrodes were heated to 550 °C for 4 hours under a nitrogen atmosphere with a heating ramp of 2.3 K min^{-1}. After the deposition, the electrodes were cleaned by a strong airstream to remove all the excess material which is not attached to the electrode surface. SEM images of C_3N_4 on glass, FTO, TiO_2, and ZnO are shown in Figure 2 and Figure S1 in the Supporting Information.

Indeed, the interactions of the hydroxy and amine groups of the CM complex precursor with the surface of the glass (SiO_2) and the FTO (F-SnO_2) direct the C_3N_4 growth, thus resulting in the formation of homogeneous and relatively organized C_3N_4 rods. Interestingly, indirect evidence for the direction of the C_3N_4 growth on the glass is given by the SEM images of the C_3N_4 powders which formed in the presence of glass (Figure 2) and in the absence of glass (see Figure S2). The regular, free C_3N_4 growth from the CM complex from water usually results in a sheet-like structure while the glass leads to a perpendicular C_3N_4 growth, presumably nucleated from the surface (XRD and FTIR data are given in Figure S3). We note that the use of different substrates to synthesize a diversity of C_3N_4 structures with organized morphologies is of great interest, but it is out of the scope of this paper. For the TiO_2 electrodes, a thin C_3N_4 layer around the particles is formed, while in the case of the ZnO particles, a polymerization of C_3N_4 around the 50 nm sized particles was observed as a result of the catalytic activity of zinc (Figure S1). For all the electrodes, the formation of carbon nitride was confirmed by EA and EDX spectroscopy (see Figure S4). The EDX data show the predominance of carbon and nitrogen atoms in all the electrodes while EA of scratched-off electrode materials disclose a C/N molar ratio of about 0.7. Moreover, we observed similar results for porous SiO_2 and ZrO_2 films. However, for the simplification of this paper only the characterization of C_3N_4 on glass, FTO, and TiO_2 are shown. The XRD patterns of the carbon nitride deposited on glass and the scratched C_3N_4/TiO_2 powder, along with the reference C_3N_4 pattern are shown in Figure 3 a. We noted that as a result of the fact that it was not possible to scratch enough material from the FTO surface, as the C_3N_4 layer was too tightly bound to the surface, we were not able to record a XRD pattern for this sample. We also faced a similar problem with the scratched C_3N_4/TiO_2 powder (most of the XRD peaks are

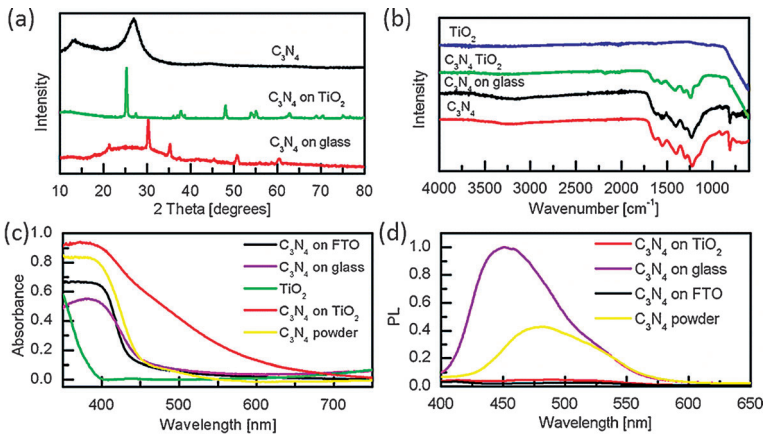

Figure 3. X-ray diffraction pattern of C_3N_4 on TiO_2 and glass (a). FTIR spectra of TiO_2, C_3N_4/TiO_2, and C_3N_4/glass (b) with respect to C_3N_4 powder. Diffuse reflectance absorption spectra (c) and emission spectra (d) of all the electrodes with respect to C_3N_4 powder.

attributed to the anatase and rutile phases of TiO_2 as shown in Figure S5) and for the C_3N_4 on glass (the heating results in the formation of crystalline SiO_2). For C_3N_4 on glass and TiO_2, at least a faint in-planar peak (at ca. 12°, index as 100) of C_3N_4 is observed. Moreover, from the diffraction pattern of the C_3N_4/TiO_2 we can rule out the formation of titanium nitride of carbide (see Figure S6). Stronger evidence for the formation of C_3N_4 on TiO_2 and glass is given by FTIR spectra (Figure 3b). The typical stretching modes of CN heterocycles were found at 1200 to 1600 cm^{-1}. Moreover, the characteristic breathing mode of the triazine units was found at approximately 800 cm^{-1}, thus indicating the formation of C_3N_4 on glass. For the C_3N_4/TiO_2, despite the strong light scattering of TiO_2 at low wavenumbers, a weak signal at 800 cm^{-1} was observed. The existence of nitrogen and carbon atoms within the TiO_2 electrode (EDX), the FTIR stretching modes, and the elemental analysis data (C/N ratio of 0.7) provide evidence for the formation of the C_3N_4 structure on TiO_2. The deposition of C_3N_4 on different substrates can influence its electronic and optical properties as a result of the different morphologies, new interfaces, and the formation of new surface states or defects within the crystal structure. The changes in the electronic properties can be monitored by the photophysical properties of the material, thus leading to changes in the intensity or the shape of the optical spectra. The UV/Vis diffuse reflectance absorbance spectra of the C_3N_4 obtained from various substrates were compared to the one that was prepared from CM only (without the presence of any substrate) and to TiO_2 powder as a reference sample (Figure 3c). The absorption spectra of the C_3N_4 which was deposited on glass and FTO are almost identical to the reference C_3N_4 powder. On the contrary, the absorption band edge of the C_3N_4/TiO_2 is strongly red-shifted, probably because of a different polymerization path of C_3N_4, a path which may lead to a change in C_3N_4 electronic states by the creation of new energy levels. In addition, the optical density, especially at longer wavelengths, increases because of multiple reflections (scattering) onto the porous surface. Images of the TiO_2 before and after carbon nitride deposition are shown in Figure S7. More evidence for the altered electronic properties manifests within the photoluminescence (PL) spectra of all C_3N_4 materials (Figure 3d). The C_3N_4 on glass exhibits an almost twofold increase in PL intensity and a more than 30 nm emission blue-shift with respect to the reference C_3N_4. The PL intensity increase indicates the formation of a better organized C_3N_4 while the PL blue-shift may result from the lack of surface states with respect to the powder. In contrast, the introduction of FTO and TiO_2 leads to a significant quenching of the PL, thus indicating that excitation energy is lost through nonradiative channels as compared to that of the powder and C_3N_4/glass, for which a large fraction of excited species deactivates through emission (a magnification of the FTO and TiO_2-C_3N_4 PL spectra is shown in Figure S8). The strong PL quenching can occur for two main reasons: 1) creation of new surface states which act as charge traps during C_3N_4 growth or 2) charge transfer from the excited C_3N_4 to the FTO and TiO_2 substrates. The absorption and the emission spectra strongly suggest that the substrate strongly influences the optical and the electronic properties of the as-synthesized C_3N_4.

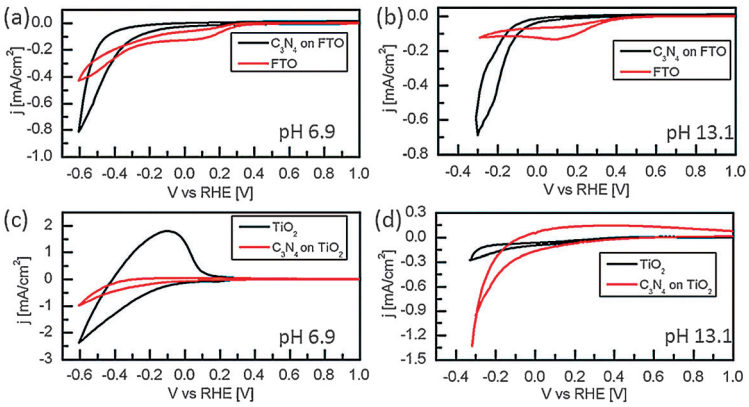

Figure 4. Cyclic voltammetry measurements of C_3N_4/FTO in 0.1 M phosphate buffer solution (a) and 0.1 M KOH solution (b). Cyclic voltammetry measurements of C_3N_4/TiO_2 in 0.1 M phosphate buffer solution (c) and 0.1 M KOH solution (d). The scan rate is 25 $mV s^{-1}$.

The pronounced catalytic activity of carbon nitride in the HER in neutral and basic solutions is shown in Figure 4. The electrodes were examined by cyclic voltammetry (CV) in 0.1M phosphate buffer solution (pH 6.9) and 0.1M KOH (pH 13.1). For the C_3N_4/FTO electrode (shown in Figure 4a,b), a catalytic current for the HER is already observed at low overpotential (with respect to RHE) at around 0.25 and 0.1 V for pH 6.9 and 13.1, respectively. These values of the metal-free catalyst are on the same order of magnitude compared to those for the state-of-the-art non-noble metal catalysts for HERs, such as Ni (see Figure S9). Moreover, under the same conditions, the reference FTO substrate shows only the substrate reduction (SnO_2 to SnO) at about 0.1 V, thus demonstrating the efficient electron transfer and superiority of the C_3N_4-coated FTO. The disappearance of this reduction peak in the presence of C_3N_4 suggests that there is no direct connection between the solution and the FTO substrate, meaning that the FTO substrate is close-to-completely covered with the C_3N_4 layer. Moreover, the current densities of the C_3N_4/FTO electrodes are impressive for a metal-free catalyst, with 0.8 mA cm^{-2} at 0.3 V and 0.6 V overpotential (with respect to RHE) for basic and neutral media, respectively. To study the stability of the C_3N_4/FTO electrodes, we measured the current voltage properties for 50 cycles using a scan rate of 25 $mV s^{-1}$. Figure S10 shows the fifth and the fiftieth scans in the two media. For both pH values, there is a negligible change in the overpotential, and about a 10% decrease of the current density at high overpotential is observed. We note that unlike neutral and basic media, the C_3N_4 electrodes were not stable under acidic conditions. Further proof of the suitability of C_3N_4 as a metal-free HER catalyst is given by the CV measurements of the C_3N_4/TiO_2 electrodes with respect to the bare TiO_2 electrode in different media (Figure 4c,d). For the bare TiO_2 electrode, a significant cathodic current is observed and is mainly related

to the accumulation of electrons within the TiO_2 and not to the HER.[21] Previous reports show that under negative potential (reduction) the observed current in neutral and acidic media is due to the reduction of the TiO_2 surface states along with accumulation of electrons within its conduction band (CB). The evidence for electron accumulation within the TiO_2 CB is given by the significant anodic peak which stands for the discharge of the accumulated TiO_2-CB electrons. Under basic conditions, most of the TiO_2 surface states are already occupied because of the basic electrolyte, so this phenomenon does not occur and only a negligible cathodic current is observed. The catalytic activity of C_3N_4 in HERs is clearly observed by measuring the CV of the C_3N_4/TiO_2 electrode. At pH 6.9, the cathodic current is reduced and the intense anodic peak significantly quenched. The strong quenching of the anodic peak implies that the cathodic current stands for electron transfer to the solution (HER) and not for electron accumulation within the TiO_2. In this medium, the overpotential for the HER is around 0.3 V and reaches a 1 $mA\,cm^{-2}$ current density at 0.6 V overpotential. The dramatic change in the TiO_2 electronic properties suggests that the C_3N_4 layer passivates its surface states, meaning that a direct electronic bonding is established. The chemical bonds are probably formed by the reaction of the hydroxy and the amine groups of the CM complex with the TiO_2 in the beginning of C_3N_4 condensation (Figure 1). The activity of the C_3N_4/TiO_2 is further increased in basic solution, thus demonstrating low overpotential (ca. 0.1 V) with notable current density (1.3 $mA\,cm^{-2}$ at 0.3 V overpotential) for metal-free electrocatalysis. The stability measurements of the TiO_2 electrodes show that the overpotential shifts slightly, and there is around a 15% decrease in the current density after 50 cycles (see Figure S11).

To further study the stability of our best systems for long terms, we measured the current voltage properties for 500 cycles using a scan rate of 25 $mV\,s^{-1}$ in basic solution. Figure S12 shows the fifth and the five hundredth scans of the two systems (C_3N_4 on FTO and TiO_2) in 0.1 M KOH. For the C_3N_4/FTO system, a full degradation of the material was observed and the substrate reduction (SnO_2 to SnO) was obtained. On the contrary, the C_3N_4/TiO_2 system demonstrates relativity high stability with about a 15% decrease in the current density along with a small shift in the overpotential (ca. 70 mV). Because of the stability and the activity of the C_3N_4/TiO_2 system we prepared a new electrode, composed from 18 nm commercial TiO_2 nanoparticles (for additional data see the Supporting Information), for higher surface area and higher conductivity. Figure S13 shows the linear sweep voltammetry (LSV) of the C_3N_4/commercial TiO_2 electrode before and after 500 CV cycles in 0.1 M KOH. The electrode demonstrated high current densities (10 mA at ~0.5 overpotential) and high stability (around ca. 10% decrease in the current density along with small shift in the overpotential ca. 80 mV).

In general, for both the C_3N_4/FTO and C_3N_4/TiO_2 systems we found better activity under basic conditions and this may be beneficial in many conversion devices such as electrolysers and fuel cells operating under alkaline conditions.[7] A Tafel analysis of the *J*-*V* curves for both FTO and TiO_2 under basic conditions (Figure S7) revealed that the HER is controlled by a Volmer–Heyrovsky mechanism (adsorption and electroreduction of H) because the Tafel slopes were practically identical to that for smooth Ni (ca. 120 $mV\,dec^{-1}$; see the Supporting Information). This data is consistent with the fact that the activity of carbon nitride in this reaction is due to its high surface amine termination (see Scheme S1). The free electrons located at the surface nitrogen atoms can easily adsorb water through a proton bridge from the solution, and as a result increase the hydrogen concentration on the surface (H_{ads}); hydrogen concentration is one of the limiting factors for HER, especially under alkaline conditions. The high amount of adsorbed hydrogen on the surface increases the probability for electron transfer and decreases the activation energy for HERs. Moreover, carbon atoms next to nitrogen atoms are positively charged because of the electron-withdrawing nitrogen atoms.[22] The positively charged carbon atom near the nitrogen atom can easily adsorb OH^- groups (left after water activation by the neighboring nitrogen atoms). The reduced H_{ads} and the hydrogen from a vicinal OH^- can recombine to form H_2. In addition, the substrate on which C_3N_4 is deposited strongly influences its activity. An energy diagram of the heterostructures developed in the present study is shown in Figure S14. From the work functions diagram, we can clearly see that the TiO_2 and C_3N_4 are forming a type II junction and consequently electrons cannot be transferred from TiO_2 to C_3N_4. This transfer indicates that the TiO_2 may only have a structural role as a high surface skeleton for the deposition of C_3N_4 and does not participate in the charge-transfer process. However, under an applied potential, the energy levels of the TiO_2 can negatively shift, thus allowing the charge transfer of electrons to the carbon nitride.

In summary, we demonstrated an efficient, easy, and generic method to generate ordered carbon nitride on different electrodes using powder coating with the cyanuric acid melamine supramolecular complex. The carbon nitride electrodes show high activity in the HER with low overpotential and acceptable current densities, which is related to an enhanced H adsorption (Volmer step). Further improvement can be achieved by different modifications of the substrates and the carbon nitride synthesis. We believe that this work opens the opportunity for a new family of materials for HERs by changing the starting complex, the substrate, and film processing. The facile deposition method enables the fabrication of many electronic and photoelectronic devices such as transistors and solar cells based on carbon nitride.

Received: October 29, 2013
Revised: December 4, 2014
Published online: February 26, 2014

Keywords: carbon nitride · electrochemistry · hydrogen · supramolecular chemistry · surface chemistry

[1] H. I. Karunadasa, C. J. Chang, J. R. Long, *Nature* **2010**, *464*, 1329–1333.
[2] W. C. Sheng, M. Myint, J. G. G. Chen, Y. S. Yan, *Energy Environ. Sci.* **2013**, *6*, 1509–1512.

[3] W. C. Sheng, H. A. Gasteiger, Y. Shao-Horn, *J. Electrochem. Soc.* **2010**, *157*, B1529 – B1536.
[4] W. F. Chen, K. Sasaki, C. Ma, A. I. Frenkel, N. Marinkovic, J. T. Muckerman, Y. M. Zhu, R. R. Adzic, *Angew. Chem.* **2012**, *124*, 6235 – 6239; *Angew. Chem. Int. Ed.* **2012**, *51*, 6131 – 6135.
[5] D. V. Esposito, S. T. Hunt, A. L. Stottlemyer, B. E. McCandless, R. W. Birkmire, J. G. Chen, *Angew. Chem.* **2010**, *122*, 10055 – 10058; *Angew. Chem. Int. Ed.* **2010**, *49*, 9859 – 9862.
[6] N. Danilovic, R. Subbaraman, D. Strmcnik, K. C. Chang, A. P. Paulikas, V. R. Stamenkovic, N. M. Markovic, *Angew. Chem.* **2012**, *124*, 12663 – 12666; *Angew. Chem. Int. Ed.* **2012**, *51*, 12495 – 12498.
[7] R. Subbaraman, D. Tripkovic, K. C. Chang, D. Strmcnik, A. P. Paulikas, P. Hirunsit, M. Chan, J. Greeley, V. Stamenkovic, N. M. Markovic, *Nat. Mater.* **2012**, *11*, 550 – 557.
[8] X. C. Wang, K. Maeda, A. Thomas, K. Takanabe, G. Xin, J. M. Carlsson, K. Domen, M. Antonietti, *Nat. Mater.* **2009**, *8*, 76 – 80.
[9] a) J. Xu, K. Shen, B. Xue, Y. X. Li, Y. Cao, *Catal. Lett.* **2013**, *143*, 600 – 609; b) J. Xu, H. T. Wu, X. Wang, B. Xue, Y. X. Li, Y. Cao, *Phys. Chem. Chem. Phys.* **2013**, *15*, 4510 – 4517.
[10] a) J. H. Sun, J. S. Zhang, M. W. Zhang, M. Antonietti, X. Z. Fu, X. C. Wang, *Nat. Commun.* **2012**, *3*, 1139; b) S. Martha, A. Nashim, K. M. Parida, *J. Mater. Chem. A* **2013**, *1*, 7816 – 7824.
[11] a) M. Shalom, S. Inal, C. Fettkenhauer, D. Neher, M. Antonietti, *J. Am. Chem. Soc.* **2013**, *135*, 7118 – 7121; b) Y. J. Cui, Z. X. Ding, P. Liu, M. Antonietti, X. Z. Fu, X. C. Wang, *Phys. Chem. Chem. Phys.* **2012**, *14*, 1455 – 1462.
[12] a) Y. Zheng, J. Liu, J. Liang, M. Jaroniec, S. Z. Qiao, *Energy. Environ. Sci.* **2012**, *5*, 6717 – 6731; b) Y. Zheng, Y. Jiao, J. Chen, J. Liu, J. Liang, A. Du, W. M. Zhang, Z. H. Zhu, S. C. Smith, M. Jaroniec, G. Q. Lu, S. Z. Qiao, *J. Am. Chem. Soc.* **2011**, *133*, 20116 – 20119; c) J. T. Jin, X. G. Fu, Q. Liu, J. Y. Zhang, *J. Mater. Chem. A* **2013**, *1*, 10538 – 10545.
[13] Y. J. Zhang, Z. Schnepp, J. Y. Cao, S. X. Ouyang, Y. Li, J. H. Ye, S. Q. Liu, *Sci. Rep.* **2013**, *50*, 3.
[14] A. Schwarzer, T. Saplinova, E. Kroke, *Coord. Chem. Rev.* **2013**, *257*, 2032 – 2062.
[15] F. Goettmann, A. Fischer, M. Antonietti, A. Thomas, *New J. Chem.* **2007**, *31*, 1455 – 1460.
[16] a) S. Stolbov, S. Zuluaga, *J. Phys. Condens. Matter* **2013**, *25*, 085507; b) Y. J. Zhang, T. Mori, J. H. Ye, M. Antonietti, *J. Am. Chem. Soc.* **2010**, *132*, 6294 – 6295.
[17] a) Y. Guo, F. Kong, C. C. Wang, S. Chu, J. C. Yang, Y. Wang, Z. G. Zou, *J. Mater. Chem. A* **2013**, *1*, 5142 – 5147; b) J. S. Zhang, X. F. Chen, K. Takanabe, K. Maeda, K. Domen, J. D. Epping, X. Z. Fu, M. Antonietti, X. C. Wang, *Angew. Chem.* **2010**, *122*, 451 – 454; *Angew. Chem. Int. Ed.* **2010**, *49*, 441 – 444.
[18] Y. Y. Bu, Z. Y. Chen, J. Q. Yu, W. B. Li, *Electrochim. Acta* **2013**, *88*, 294 – 300.
[19] S. B. Yang, X. L. Feng, X. C. Wang, K. Mullen, *Angew. Chem.* **2011**, *123*, 5451 – 5455; *Angew. Chem. Int. Ed.* **2011**, *50*, 5339 – 5343.
[20] Y. S. Jun, E. Z. Lee, X. C. Wang, W. H. Hong, G. D. Stucky, A. Thomas, *Adv. Funct. Mater.* **2013**, *23*, 3661 – 3667.
[21] a) F. Fabregat-Santiago, I. Mora-Sero, G. Garcia-Belmonte, J. Bisquert, *J. Phys. Chem. B* **2003**, *107*, 758 – 768; b) T. Berger, T. Lana-Villarreal, D. Monllor-Satoca, R. Gomez, *J. Phys. Chem. C* **2007**, *111*, 9936 – 9942.
[22] Y. Zhao, R. Nakamura, K. Kamiya, S. Nakanishi, K. Hashimoto, *Nat. Commun.* **2013**, *4*, 2390.

